



Contents lists available at ScienceDirect

Materials Science in Semiconductor Processing

journal homepage: www.elsevier.com/locate/mssp

Ion-beam synthesis and thermal stability of highly tin-concentrated germanium – tin alloys

Tuan T. Tran^{a,*}, Hemi H. Gandhi^b, David Pastor^b, Michael J. Aziz^b, J.S. Williams^a^a Department of Electronic Materials Engineering, Research School of Physics and Engineering, Australian National University, Canberra, ACT 0200, Australia^b Harvard John A. Paulson School of Engineering and Applied Sciences, Cambridge, MA 02138, USA

ARTICLE INFO

Keywords:

Germanium-tin alloys
 Ion implantation
 Semiconductor processing
 Direct bandgap group IV alloys

ABSTRACT

A 9 at% Sn Ge-Sn alloy of good crystalline quality has been achieved by ion implantation followed by pulsed laser melting and resolidification. The concentration and crystallinity of the alloys are fully characterised by Rutherford backscattering spectrometry, X-ray diffraction, transmission electron microscopy and Raman spectroscopy. At high Sn concentrations, oxygen intermixing from a capping oxide layer, which is used to prevent ion-beam induced porosity, can interfere with the solidification process and compromise overall crystal quality. This indicates that the near surface layer containing oxygen after ion implantation must be removed before pulsed laser melting in order to obtain good crystal quality. The alloy's crystallinity is thermally stable under annealing up to 400 °C for 30 min. This thermal budget is comparable to that of Ge-Sn produced by conventional MBE or CVD methods and suitable for subsequent device fabrication and post-processing.

Over the last few years the semiconductor research community has directed considerable effort towards developing group IV germanium-tin (Ge-Sn) binary alloys. This interest in the Ge-Sn material platform stems from its attractive high performance optoelectronic properties and its potential deployment to solve long-anticipated problems in front-end-of-line (FEOL) and back-end-of-line (BEOL) electronic device processing. Ge-Sn alloy (11 at% Sn) has been calculated to have four times higher carrier mobility compared to non-alloyed Ge, indicating high suitability for FEOL transistors [1]. For newly proposed tunnel field effect transistors, use of fundamental direct bandgap semiconductor like the Ge-Sn alloy could enhance tunnelling probability and related drive-current, allowing operation of devices beyond theoretical subthreshold slope limitations of 60 mV/dec [2,3]. For BEOL structure and data communication, the prospect of transmitting signals using photons is tantalising for ultimate speed and low power consumption. To facilitate this, there has been much effort in integrating photonic materials, like direct bandgap III-V semiconductors, into Si CMOS circuitry. For example, the first end-to-end silicon photonics integrated link operated at 50 Gbits⁻¹ over a single fibre has been demonstrated by Intel's Photonics Technology Labs [4]. While this result was promising, it relied on cumbersome III-V bonding of an indium phosphide layer to a silicon photonic chip. An alternative, potentially lower cost solution would be to use Si CMOS compatible direct bandgap semiconductor like Ge-Sn alloys for light emission. A

proof-of-concept optically pumped laser from a Ge-Sn alloy has been demonstrated, where the material was grown directly on a silicon substrate by a chemical vapour deposition technique (CVD) [5].

Recently, Ge-Sn alloys have also been produced by ion beam synthesis using ion implantation and nanosecond pulsed laser melting (PLM) [6,7]. This fabrication method is potentially advantageous over standard Ge-Sn fabrication via CVD in that it may allow for higher Sn fraction, easier post fabrication pathway for layer lattice relaxation and device implementation. A single crystalline Ge-Sn alloy with ~6 at. % Sn has been achieved using this method, with excellent crystal quality except for some local pore formation that occurs after ion implantation [7]. These defective regions have been shown to be a consequence of ion-beam induced porosity in Ge, which also increases the loss of Sn during implantation [8]. By using a nanometer scale pre-implantation capping layer of silicon dioxide (SiO₂), the porosity and Sn loss due to sputtering are both significantly suppressed as shown in Ref. [8]. After implantation, a Sn content of ~15 at% has been achieved for a Ge substrate with a 40 nm capping layer. No sign of surface porosity can be detected in these samples.

Developed from the work in Ref. [8] which focused mostly on the suppressing effect of the capping layer, this work presents the fabrication aspect of the Ge-Sn alloys with detailed physical characterisation including Rutherford backscattering spectrometry (RBS), X-ray diffraction (XRD), transmission electron microscopy (TEM) and Raman

* Corresponding author.

E-mail address: tuan.tran@anu.edu.au (T.T. Tran).<http://dx.doi.org/10.1016/j.mssp.2016.10.049>

Received 5 September 2016; Received in revised form 23 October 2016; Accepted 26 October 2016

Available online xxxx

1369-8001/ © 2016 Elsevier Ltd. All rights reserved.

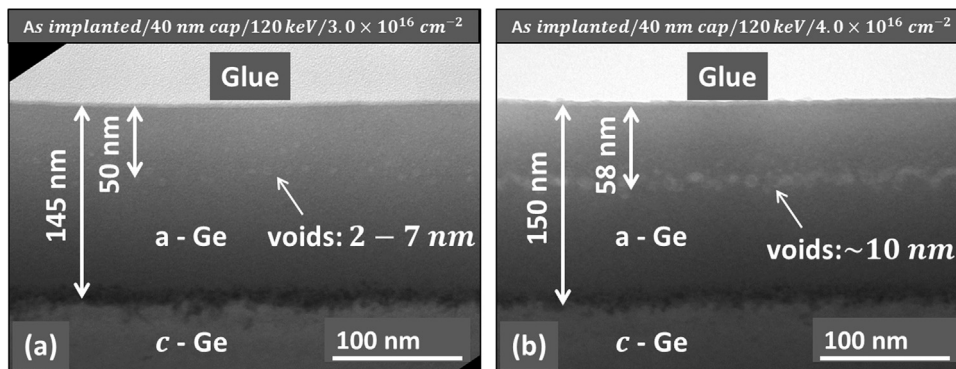


Fig. 1. TEM micrographs of the as-implanted samples at the dose of $3.0 \times 10^{16} \text{cm}^{-2}$ (Fig. 1(a)) and $4.0 \times 10^{16} \text{cm}^{-2}$ (Fig. 1(b)). In Fig. 1(a), a band of nanometer scale voids occurred at the depth of the maximum vacancy production. This band grows larger with higher implant dose in Fig. 1(b).

spectroscopy. Furthermore, the thermal stability of the alloys, which is crucial information for further application of the materials, will also be presented in this contribution.

Prior to ion implantation, several p-type (Ga doped) (100) Ge substrates were coated with a $\sim 40 \text{ nm}$ SiO_2 by plasma enhanced chemical vapour deposition. The capped substrates were implanted with $^{120}\text{Sn}^-$ at an energy of 120 keV and the implant doses were in the range of $2.5 - 4.5 \times 10^{16} \text{cm}^{-2}$. All the substrates were misoriented 7° to the [100] crystal axis of the substrate to minimise channelling, and also were kept at liquid nitrogen temperature (LN_2T) to suppress ion-beam-induced porosity [9,10].

Fig. 1 shows the TEM micrographs of the Ge substrates after the implantation of Sn and after the removal of the capping oxide layer by hydrofluoric acid (HF). The effectiveness of the capping layer in preventing porosity is clearly shown in Fig. 1(a) and (b), where the surface remains atomically flat surface. However, it is worth noting that at the depth of 50 nm below the surface there is a band of voids measured from 2 nm to 7 nm in the $3.0 \times 10^{16} \text{cm}^{-2}$ sample (Fig. 1(a)). Beyond the dose of $3.0 \times 10^{16} \text{cm}^{-2}$, the size of the voids increases to $>10 \text{ nm}$ at a higher implant dose of $4.0 - 4.5 \times 10^{16} \text{cm}^{-2}$ (Fig. 1(b)). Further investigation will be presented later to clarify whether this band of voids can be annihilated by a PLM process. Subsequently, PLM was achieved using a frequency tripled Nd: YAG laser (355 nm , 4 ns) with a single pulse of $\sim 0.4 \text{ J cm}^{-2}$. During the process, time resolved reflectivity measurements performed with an Ar ion (488 nm) laser source provided a melt duration of $53 - 66 \text{ ns}$. Crystal quality of the samples are characterised by Rutherford backscattering spectrometry (RBS), X-ray diffraction (XRD), Raman spectroscopy and transmission electron microscopy (TEM).

After PLM, RBS spectra were taken on the $3.0 \times 10^{16} \text{cm}^{-2}$ and $4.0 \times 10^{16} \text{cm}^{-2}$ samples in channelling and random configurations to characterise the physical properties of the samples after PLM. The probing beam of the RBS system is $^4\text{He}^+$ at an energy of 2 MeV . The Sn concentration of the $3.0 \times 10^{16} \text{cm}^{-2}$ sample after implantation is $\sim 9.5 \%$ as determined by fitting the red spectrum in Fig. 2(a) with a simulated RUMP spectrum [11]. The Sn profile of the sample is Gaussian-like as expected for a non-porous Ge sample. After PLM, the crystal structure of the Ge-Sn layer recovered very well as indicated by the reduced scattering yield of the green spectrum. By comparing random and channelled RBS spectra, the substitutionality of Sn atoms is calculated to be $85 - 90\%$. Although the Sn profile has been redistributed slightly during PLM, the peak concentration of Sn in Ge is estimated to be $\sim 9\%$. This result is certainly encouraging as it is comparable to some of the best studies using molecular beam epitaxy [12,13] and chemical vapour deposition [14,15]. For the $4.0 \times 10^{16} \text{cm}^{-2}$ sample, the high scattering yield of the channelling spectrum (purple) represents a disordered layer, noting the two large bumps: one at the sample's surface and one at about the back edge of the amorphous layer. These two features will be clarified in the following TEM figures.

Fig. 2(b) is an X-ray reciprocal space map of the $3.0 \times 10^{16} \text{cm}^{-2}$ sample after PLM. The map was constructed by doing a series of $\omega - 2\theta$ scans at slightly different ω offsets around the asymmetric reciprocal point ($\bar{2}24$). This asymmetrical mapping is able to show the in-plane (Q_x) as well as the out-of-plane lattice expansion (Q_y), so that any strain relaxation can be observed. At the cross of the figure is the reciprocal point ($\bar{2}24$) from the substrate. The perfectly vertical streak going downwards from the substrate's point is from the compressively strained Ge-Sn layer. This result of strain is usually expected for good epitaxy of a thin layer in which there is uniaxial strain perpendicular to the film as a result of the film accommodating the same lateral lattice parameter as the substrate. However, studies have shown that the biaxial compressive strain as in this case has a negative impact in the Ge-Sn layer in terms of the direct bandgap transition as it requires a higher concentration of Sn to compensate for the strain [16].

Further TEM analysis was again undertaken to characterise the crystallinity of the Ge-Sn layer after PLM. Fig. 3(a) shows that the small band of $2 - 7 \text{ nm}$ voids in Fig. 1(a) can be annihilated by the PLM process for the $3.0 \times 10^{16} \text{cm}^{-2}$ case. No significant disorder and extended defects have been observed in this sample. Electron diffraction conducted within the Ge-Sn layer of this sample (inset) shows a typical pattern of a diamond cubic structure. The blurry ring within the pattern was identified to be from an amorphous platinum layer deposited on the Ge samples during focused-ion-beam sample preparation. However, for the higher dose case in Fig. 1(b) it is shown in Fig. 3(b) that the voids and impurities following implantation give rise to residual disorder after PLM in the form of large amorphous regions. Our energy-dispersive X-ray spectroscopy data show that the relative concentration of Sn changes only slightly within these regions; i.e. these blobs are not Sn precipitates. Meanwhile, the concentration of oxygen (O) significantly increases as indicated by an EDX scan across the blobs. Therefore, it is hypothesised that O atoms in the capping layer are intermixed with the substrate during the implantation. Although the intermixing layer is shallow, within 5 nm of the surface, O appears to be relocated towards the voids during the melting stage, thus hindering a full recovery of the lattice. Similarly, the intermixed oxygen appears to retard the recrystallization at the sample's surface as shown in the upper part of the Fig. 3(b)'s inset. The amorphous regions at the surface and close to the back edge of the Ge-Sn layer are consistent with the two large bumps in the RBS spectrum mentioned previously. It is therefore necessary to remove at least the first 5 nm of the sample's surface prior to PLM by a controlled etching process such as reactive ion etching to remove the intermixed O and achieve a better quality crystalline alloy layer.

Raman spectroscopy of post-PLM samples are conducted to study bonding arrangements within the Ge-Sn lattice, most noticeably the Ge-Sn local vibration phonon mode and the 1st order Ge-Ge phonon mode (Fig. 4). This Raman spectroscopy was performed using a Renishaw 2000 micro-Raman instrument with a red laser source

Download English Version:

<https://daneshyari.com/en/article/5006177>

Download Persian Version:

<https://daneshyari.com/article/5006177>

[Daneshyari.com](https://daneshyari.com)